Catalysis Letters, Vol. 117, Nos. 3–4, September 2007 (© 2007)
DOI: 10.1007/s10562-007-9122-9

Oxidative dehydrogenation of ethane over Co–$BaCO_3$ catalysts using CO_2 as oxidant: effects of Co promoter

Xin Zhang,* Qing Ye, Boqing Xu, and Dehua He

Department of Chemistry, Tsinghua University, Beijing, 100084, P.R. China

Received 11 April 2007; accepted 11 April 2007

Co–$BaCO_3$ catalysts exhibited high catalytic performance for oxidative dehydrogenation of ethane (ODE) using CO_2 as oxidant. The maximal formation rate of C_2H_4 was 0.264 $\text{mmol}\cdot\text{min}^{-1}\cdot(\text{g}\cdot\text{cat.})^{-1}$ (48.0% C_2H_6 conversion, 92.2% C_2H_4 selectivity, 44.3% C_2H_4 yield) on 7 wt% Co–$BaCO_3$ catalyst at 650 °C and 6000 ml. $(\text{g}\cdot\text{cat.})^{-1}$. h^{-1}. Co–$BaCO_3$ catalysts were comparatively characterized by XRF, N_2 isotherm adsorption-desorption, XRD, H_2-TPR and LRs. It was found that Co^{4+}–O species were active sites on these catalysts in ODE with CO_2. The redox cycle of Co–O species played an important role on the catalytic performance of Co–$BaCO_3$ catalysts. On the other hand, the co-operation of $BaCO_3$ and $BaCoO_3$ was considered to be one of possible reasons for the high catalytic activity of these catalysts.

KEY WORDS: oxidative dehydrogenation; Co–$BaCO_3$; ethane; ethene; CO_2.

1. Introduction

Oxidative dehydrogenation of ethane (ODE) is one of important processes for producing ethene. However, it is still hard challenge to obtain the high selectivity and yield of ethene in this reaction. ODE using CO_2 as oxidant provides an alternative rout for reaching the high selectivity of ethene, because CO_2 is expected (1) to eliminate the flammability of reactants, (2) to enhance dehydrogenation of ethane to ethene and reduce over-oxidation of ethene, (3) to maintain the catalytic activity by removing coke forming on catalysts, and (4) to be inexpensive and available in great amount, etc [1–3].

Up to date, a great deal of effort has been made to develop effective catalyst for ODE with CO_2, such as supported Cr-oxide catalysts, Ga-based catalysts, Na_2WO_4–Mn/SiO_2 catalysts, CaO–CeO_2 catalysts, Mo_2C/SiO_2 catalysts, etc [1–22]. Table 1 summarizes the catalytic performance and reaction conditions of topical catalysts for ODE with CO_2. In order to obtain better catalytic reactivity, it is highly desirable to develop new catalyst and/or carry out the modification of these catalysts.

In this present work, Co–$BaCO_3$ catalysts have been applied for ODE with CO_2. We have found that Co–$BaCO_3$ catalysts exhibited high catalytic performance in the reaction. In order to establish the relation of their catalytic performance with Co species, we have characterized the physicochemical properties of Co–$BaCO_3$ catalysts by XRF, N_2 isotherm adsorption-desorption, XRD, H_2-TPR and LRs.

2. Experimental

2.1. Catalysts preparation

Co–$BaCO_3$ catalysts with different Co content were prepared by aqueous solution impregnation method. Under constant and quick stirring, $BaCO_3$ powder (Beijing Hongxin Chemical, A.R.) was added to $Co(NO_3)_2$ ($Co(NO_3)_2\cdot 6H_2O$, Beijing Shuanghuan Chemical, A.R.) aqueous solution. The volume of $Co(NO_3)_2$ aqueous solution was ca. 1.5 times more than that of $BaCO_3$ powder. The mixture was evaporated at 90 °C under reduced pressure for 4 h. Subsequently, it was calcined at 350 °C for 3 h and 750 °C for 6 h in air flow.

2.2. Catalytic test

Oxidative dehydrogenation of C_2H_6 with CO_2 was carried out in a continuous-flow fixed-bed quartz reactor (i.d. = 10 mm) mounted inside a tube furnace. The space up and down the catalyst bed (0.5 g, 20∼40 mesh) in the reactor was filled with quartz wool to suppress gas-phase homogenous reaction. The catalyst was firstly heated to reaction temperature in CO_2 flow, and then exposed to the feed ($C_2H_6/CO_2 = 1/3$; C_2H_6: 99.99%; CO_2: 99.995%; Beijing Huayuan Gas). The feed and products were analyzed by an on-line gas chromatograph (Angilent 1490 GC) with TDX-01 column (TCD, Ar carrier, 99.999%) for the separation of H_2, CH_4, CO, CO_2, C_2H_4 and C_2H_6. The experimental data were corrected after the reaction for 1 h. Water in the outlet gas was collected by a cold trap (−55 °C). Reactants conversion, products selectivity and products yield were calculated as,

---

*To whom correspondence should be addressed.
E-mail: zhangxinzhangcn@yahoo.com.cn

1011-372X/07/0900–0140/0

Table 1
Catalytic performance and reaction conditions of the typical catalysts for ODE with CO_2

Catalyst	T (°C)	Space velocity ($ml \cdot h^{-1} \cdot (g \cdot cat.)^{-1}$)	C_2H_6/CO_2 ratio	Conversion (%)		Selectivity (%)	Yield (%)	Ref.
				C_2H_6	CO_2	C_2H_4	C_2H_4	
Ga_2O_3	650	9000	5/25	19.6		94.5	18.6	[4]
1.5%K-5.5%Cr-17%MnO_2/SiO_2	830	3600[a]	1/1.5	82.6	55.7	72.8	60.1	[6]
6 wt% Cr_2O_3/SiO_2–SO_4^{2-}	650	3600	1/5	67.2	21.9	81.8	55.0	[7]
9Fe-9 Mn /Si-2	800	1000[a]	1/1	68.6	39.1	92.3	63.3	[14]
Na_2WO_4–Mn/SiO_2	800	3600[a]	1/1	69.5		90.0	62.5	[16]
CaO–CeO_2	750	12000	1/2	24.2		91.0	22.0	[19]
Cr/HZSM-5 ($SiO_2/Al_2O_3 = 1900$)	650	6000	1/9	68.2	69.5	90.0	61.4[b]	[20]
Cr-MCM-41	7000	61[a]	1/2	51.2		94.5	48.4	[21]
Cr/TS-1(150)	650	9000	12/48	62.2	17.2	81.0	50.4	[22]

[a] The unite of space velocity is h^{-1}.

C_2H_6 Conversion % = $(2n_{C_2H_4} + n_{CH_4})/(2n_{C_2H_6} + 2n_{C_2H_4} + n_{CH_4})$

CO_2 Conversion % = $n_{CO}/(n_{CO_2} + n_{CO})$

C_2H_4Selectivity % = $n_{C_2H_4}/(2n_{C_2H_4} + n_{CH_4})$

C_2H_4 Yield % = C_2H_6 Conversion × C_2H_4 Selectivity

The conversion of ethane to coke was neglected because the instantaneous formation of coke was dependent on reaction time and difficult to estimate.

Formation rate of ethene (F.R.) and turnover frequency of ethene (TOF) were respectively calculated as,

Formation rate of ethene ($mmol \cdot min^{-1} \cdot (g \cdot cat.)^{-1}$) = $W_{C_2H_4} \times F_{total}$/(g. catalyst)

Turnover frequency of ethene ($mol \cdot min^{-1} \cdot (mol \cdot$ Co-atom$)^{-1}$) = $W_{C_2H_4} \times F_{total}/M_{Co\text{-}atom}$ where $W_{C_2H_4}$ is the concentration of C_2H_4 in outlet gas obtained by GC analysis (%), F_{total} is the flow rate of feed gas ($mol \cdot min^{-1}$), and $M_{Co\text{-}atom}$ is the amount of Co atoms in the catalyst (mol).

2.3. Characterization

Co content (wt%) in Co–$BaCO_3$ catalysts was measured by Rogaku Rotflex 3013 X-ray fluorescence (XRF) instrument with W target operated at 40 kV and 50 mA.

Specific surface area (S_{BET}) of these catalysts was characterized by N_2 isothermal adsorption-desorption method. N_2 isothermal adsorption-desorption experiment was performed at the temperature of liquid nitrogen by Micromeritics ASAP400 adsorptionmeter. The catalyst (ca. 240 mg) was degassed at 200 °C and 10^{-6}Torr before the measurement of data.

Bulk structure of these catalysts was identified by Rogaku Rotflex D/Max-C powder X-ray diffractometer (XRD) with Cu $K\alpha$ radiation (λ = 0.15046 nm) operated at 40 kV and 30 mA.

LR spectrum (LRs) of these catalysts was recorded at room temperature by Renishaw RM1000 confocal microprobe Raman spectrometer equipped with He^+/Ne^+ laser. The laser was operated at frequency of 514 nm and at a power of 15 mW.

H_2 temperature-programmed reduction (H_2-TPR) experiment of these catalysts was carried out by home-built fixed-bed TPR apparatus. The catalyst (ca. 200 mg) was pretreated by 30 $ml \cdot min^{-1}$ air flow at 750 °C for 1 h, and then purged with 20 ml/min He flow. In H_2-TPR experiment, the catalyst was exposed to 5%v H_2/N_2 flow with a rate of 20 $ml \cdot min^{-1}$, and heated from r. t. to 850 °C with a rate of 10 $°C \cdot min^{-1}$. Water was removed from the outlet gas with a cold trap at −85 °C to avoid its interference with TCD detector.

3. Results and discussion

3.1. Catalytic performance

Table 2 lists catalytic performance of Co–$BaCO_3$ catalysts in ODE with CO_2 at 650 °C and 6000 ml $h^{-1} \cdot (g \cdot cat.)^{-1}$. Firstly, we investigated the gas-phase homogeneous reaction of ethane with CO_2 in blank reactor under the reaction conditions. Ethane conversion was 2.4% and CO_2 conversion was nearly zero in the blank reactor. When quartz wool was filled in the reactor, ethane conversion further decreased. These results indicate that the homogenous reaction between ethane and CO_2 could be negligible under the reaction conditions.

$BaCO_3$ showed 3.2% ethane conversion and 1.5% CO_2 conversion, suggesting that $BaCO_3$ had low catalytic activity in ODE with CO_2. Comparing with $BaCO_3$, Co–$BaCO_3$ catalysts exhibited distinctively high catalytic activity in the reaction. With the increase of Co content in theses catalysts, ethane conversion and CO_2 conversion gradually increased while ethene selectivity decreased. The formation rate of ethene reached the maximum value 0.264 $mmol \cdot min^{-1} \cdot (g \cdot cat.)^{-1}$ on 7 wt% Co–$BaCO_3$ catalyst with the increase of Co content. These results suggest that the presence of Co in

Table 2
Catalytic performance of Co–$BaCO_3$ catalysts for oxidative dehydrogenation of ethane with CO_2 as oxidant[a]

Catalyst[b]	S_{BET}(m^2/g)	Conversion (%)		Selectivity (%)		CO/H_2	Yield $_2H_4$(%)	F.R.[c] (mmol · min^{-1} · (g · cat.)$^{-1}$)
		C_2H_6	CO_2	C_2H_4	CH_4			
Blank reactor	–	2.4	–	97.2	2.8	–	2.3	–
Quartz wool	–	1.1	–	99.5	0.5	–	1.1	–
$BaCO_3$	37.9	3.2	1.5	99.0	1.0	–	3.2	0.022
3 wt% Co–$BaCO_3$	22.6	26.8	10.7	98.2	1.8	1.1	26.3	0.171
7 wt% Co–$BaCO_3$	6.9	48.0	16.6	92.2	7.8	1.2	44.3	0.264
10 wt% Co–$BaCO_3$	5.5	50.4	18.7	87.5	12.5	1.6	44.1	0.259
13 wt% Co–$BaCO_3$	5.1	58.5	21.0	68.4	31.6	2.1	40.0	0.218

[a] Reaction conditions: 650 °C, SV = 6000 ml · h^{-1} · (g · cat)$^{-1}$, $C_2H_6/CO_2 = 1/3$.
[b] Co-content in the catalyst was estimated from XRF data.
[c] F.R. denotes the formation rate of C_2H_4 on these catalysts in ODE with CO_2.

Co–$BaCO_3$ catalysts plays great roles on the observed catalytic reactivity of these catalysts.

Effects of space velocity on the catalytic performance of 7 wt% Co–$BaCO_3$ catalyst were investigated (figure 1). The smaller space velocity caused the higher conversion of ethane and CO_2 as well as the lower selectivity of ethene. In addition, the formation rate of ethene increased with the decrease of space velocity, implying that the desorption and diffusion of ethene from the catalyst affected the catalytic performance of the catalyst.

Catalytic stability of 7 wt% Co–$BaCO_3$ catalyst at 650 °C is shown in figure 2. At initial reaction stage (~ ca. 60 min), ethane conversion slightly decreased while ethene selectivity increased with the increase of time on stream. The phenomenon is due to the formation of coke on the catalyst at the initial reaction stage. Afterwards (60~300 min), ethane conversion and ethene selectivity were almost stable. The formation rate of ethene was slightly fluctuant in the investigated reaction time. These results demonstrate that 7 wt% Co–$BaCO_3$ exhibited stable catalytic reactivity in ODE with CO_2 after the short initial reaction stage.

3.2. Characterization

It can be seen in table 2, specific surface area (S_{BET}) of Co–$BaCO_3$ catalysts was lower than that of $BaCO_3$, and it slightly reduced with the increase of Co content. Figure 3 shows XRD patterns of Co–$BaCO_3$ catalysts and reveals the structure and composition of these catalysts. The addition of Co into these catalysts led to the formation of pervoskite $BaCoO_3$ (2θ = 26.2, 29.5, 32.0 and 42.0). Co_3O_4, Co_2O_3 and CoO were not detected in these catalysts. These results show that $BaCO_3$ and $BaCoO_3$ were main component in Co–$BaCO_3$ catalysts.

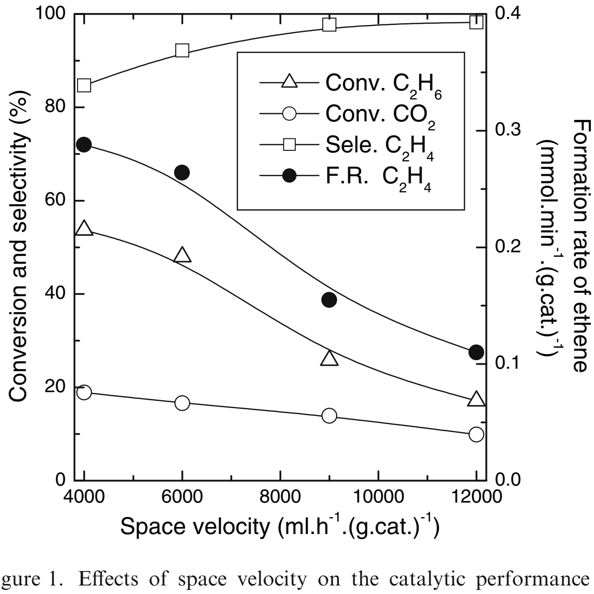

Figure 1. Effects of space velocity on the catalytic performance of 7 wt% Co–$BaCO_3$ catalyst in ODE with CO_2. Reaction conditions: 650 °C and $C_2H_6/CO_2 = 1/3$.

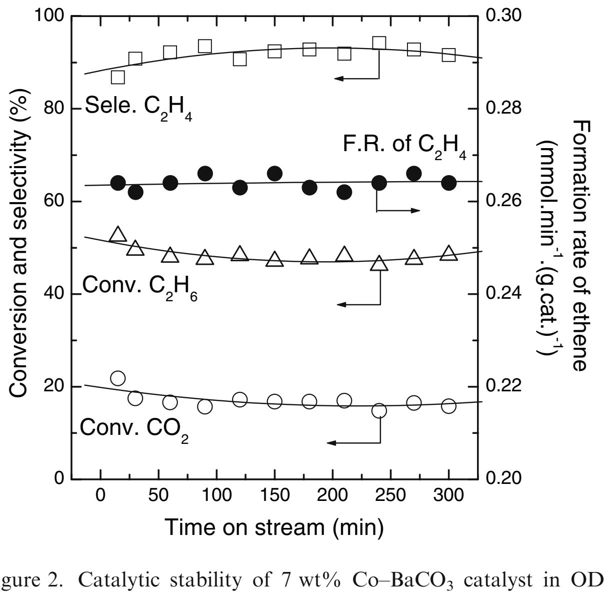

Figure 2. Catalytic stability of 7 wt% Co–$BaCO_3$ catalyst in ODE with CO_2 Reaction conditions: 650 °C, 6000 ml · h^{-1}. (g · cat.)$^{-1}$ and $C_2H_6/CO_2 = 1/3$.

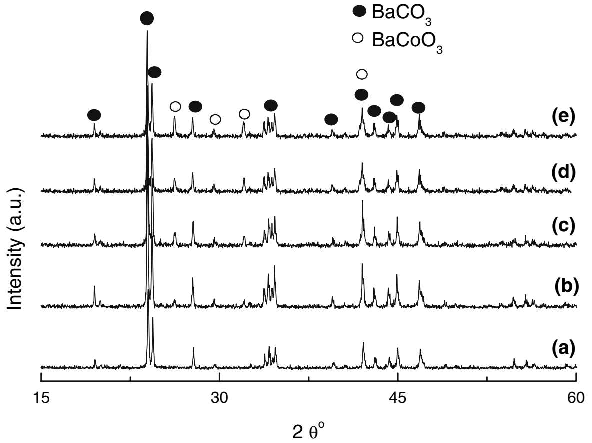

Figure 3. XRD patterns of Co–$BaCO_3$ catalysts, (a) $BaCO_3$, (b) 3 wt% Co–$BaCO_3$, (c) 7 wt% Co–$BaCO_3$, (d) 10 wt% Co–$BaCO_3$, (e) 13 wt% Co–$BaCO_3$.

On the other hand, $I_{BaCoO_3(101)}/I_{BaCO_3(111)}$ ratio is used to roughly express the content of $BaCoO_3$ in these catalysts, where $I_{BaCoO_3(101)}$ and $I_{BaCO_3(111)}$ are respectively the intensity of XRD peak at $2\theta = 26.2$ and $2\theta = 23.9$. The content of $BaCoO_3$ was smaller than that of $BaCO_3$ in Co–$BaCO_3$ catalysts, and it gradually increased with Co content increasing (table 3).

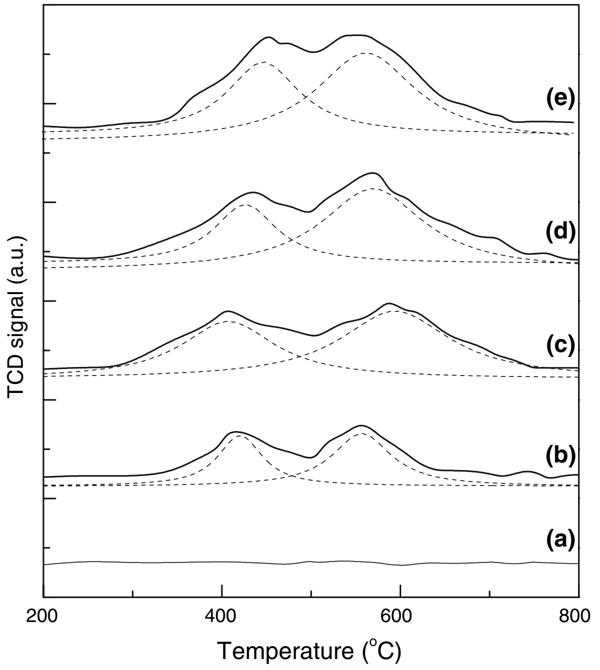

Figure 4. H2-TPR profiles of Co–$BaCO_3$ catalysts, (a) $BaCO_3$, (b) 3 wt% Co–$BaCO_3$, (c) 7 wt% Co–$BaCO_3$, (d) 10 wt% Co–$BaCO_3$, (e) 13 wt% Co–$BaCO_3$.

Figure 4 presents H_2-TPR profiles of Co–$BaCO_3$ catalysts and the results of H_2-TPR are summarized in table 3. $BaCO_3$ could not cause the erroneous interpretation of H_2-TPR profiles, because $BaCO_3$ decomposes at ca. 920 °C that is above the temperature range of the H_2-TPR studies. No reduction peak was detected on $BaCO_3$. Two clear reduction peaks at 410~450 °C and 550~580 °C were observed in Co–$BaCO_3$ catalysts; in addition, H_2 consumption of the low-temperature reduction peaks (410~450 °C) was as similar as that of the corresponding high-temperature reduction peaks (550~580 °C). Pyartuitsky *et al.* [23] found that $SrCoO_3$ exhibited two H_2-TPR reduction peaks at about 477 and 517 °C which were attributed to the reduction of $Co^{4+} \rightarrow Co^{2+} \rightarrow Co^0$. Dai *et al.* [24] detected two reduction peaks at 482 and 800 °C in H_2-TPR of $SrCoO_{3-0.401}$, due to the two reduction steps of Co^{4+}. Therefore, we tentatively assign the two reduction peaks observed in H_2-TPR of Co–$BaCO_3$ catalysts to the stepwise reduction of $Co^{4+} \rightarrow Co^{2+} \rightarrow Co^0$. In addition, H_2 consumption of Co–$BaCO_3$ catalysts gradually increased with the increase of Co content, suggesting that the amount of the reducible Co species increased.

Table 3

Physicochemical properties of Co–$BaCO_3$ catalysts

Catalyst	$I_{BaCoO_3(101)}/I_{BaCO_3(111)}$ (XRD)	H_2 consumption (H_2-TPR) $(mmol\cdot(g\cdot cat.)^{-1})$	
		410~450 °C	550~580 °C
$BaCO_3$	–	–	–
3 wt% Co–$BaCO_3$	0.02	0.43	0.47
7 wt% Co–$BaCO_3$[a]	0.07	1.08	1.18
10 wt% Co–$BaCO_3$	0.11	1.17	1.40
13 wt% Co–$BaCO_3$	0.17	1.67	2.00

Figure 5 gives LR spectra of $BaCO_3$ and 7 wt% Co–$BaCO_3$ catalyst treated under different conditions. $BaCO_3$ appeared Raman bands at 131, 148 and 690 cm^{-1}, which are respectively due to *v*Ba–O (131 and 148 cm^{-1}) [25–27] and the binding in-plane vibration of CO_3^{2-} (690 cm^{-1}) [28–29]. LR spectra of Co_3O_4, Co_2O_3 and CoO as references are shown in figure 6. 7 wt% Co–$BaCO_3$ catalyst did not appeared the characteristic

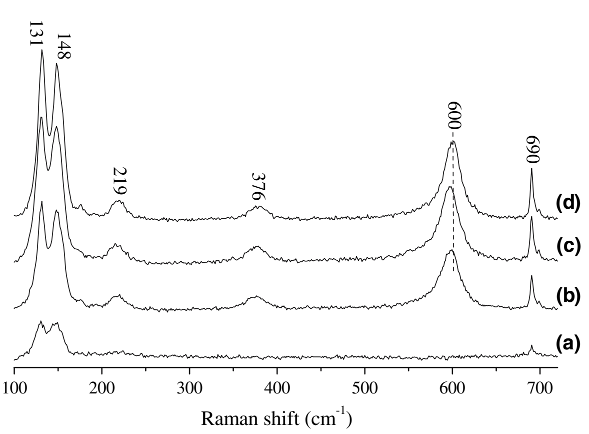

Figure 5. LR spectra of (a) $BaCO_3$, (b) fresh 7 wt% Co–$BaCO_3$ catalyst, (c) 7 wt% Co–$BaCO_3$ catalyst treated by ethane at 650 °C for 1 h, (d) 7 wt% Co–$BaCO_3$ firstly treated by ethane at 650 °C for 1 h and then by CO_2 at 650 °C for 1 h.

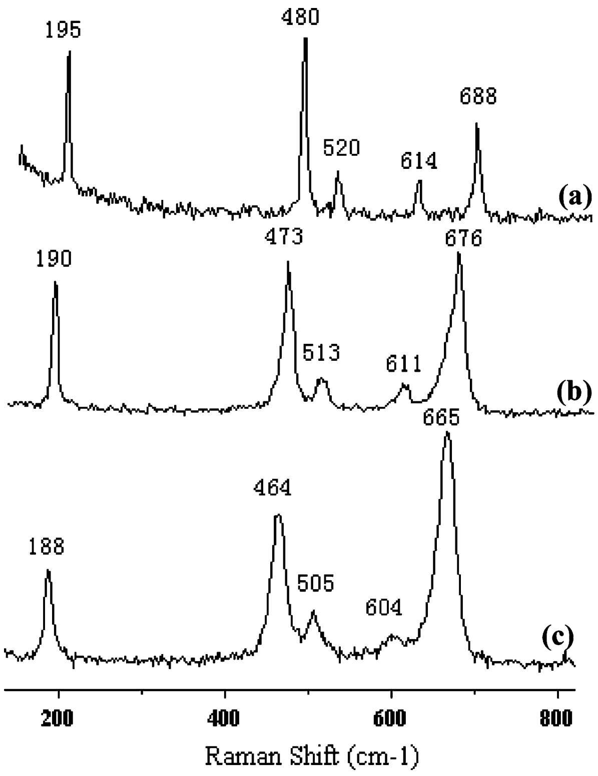

Figure 6. LR spectra of (a) Co_3O_4, (b) Co_2O_3 and (c) CoO.

Raman bands of Co_3O_4, Co_2O_3 and CoO, indicating that there were not Co_3O_4, Co_2 O_3 and CoO in the catalyst. Comparing with $BaCO_3$, Co_3O_4, Co_2O_3 and CoO, Co–$BaCO_3$ catalysts presented new Raman bands at 600, 376, 219 cm^{-1}, which are assigned to νCo^{4+}–O originating from $BaCoO_3$ [30–31]. H_2-TPR peaks of the catalyst probably arise from the reaction of H_2 with these Co–O species. It is deduced that oxygen species bonding to Co^{4+} were removed by ethane and then CO_2 oxidized the reduced Co^{n+}–O ($n < 4$) species to Co^{4+}–O species in ODE with CO_2.

3.3. *TOF and apparent activation energy*

In order to further investigate the catalytic performance of Co–$BaCO_3$ catalysts, turnover frequency of ethene (TOF) and apparent activation energy of the reaction (Ea) on $BaCO_3$ and 7 wt% Co–$BaCO_3$ catalyst were comparatively studied. Figure 7 shows Arrhenius plots for ODE with CO_2 on these catalysts. 7 wt% Co–$BaCO_3$ catalyst exhibited higher TOF than $BaCO_3$ in the reaction. TOF gradually increased on 7 wt% Co–$BaCO_3$ catalyst with the increase of the reaction temperature. Ea is ca. 135 $kJ \cdot mol^{-1}$ on 7 wt% Co–$BaCO_3$ catalyst while Ea is 192 $KJ \cdot mol^{-1}$ on $BaCO_3$. Therefore, 7 wt% Co–$BaCO_3$ had higher catalytic reactivity than $BaCO_3$ in ODE with CO_2. These results indicate that Co species have important roles on the catalytic reactivity of 7 wt% Co–$BaCO_3$ catalyst, which are agreement with those results of catalytic test.

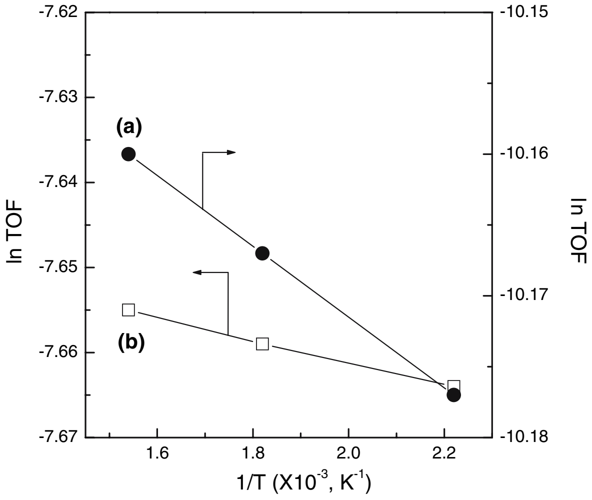

Figure 7. Arrhenius plots for ODE with CO_2 on (a) $BaCO_3$ and (b) 7 wt% Co–$BaCO_3$ catalyst.

These above results demonstrate that the presence of Co species modifies the properties of Co–$BaCO_3$ catalyst which in turn determines the catalytic performance of these catalysts. Highly reactive 7 wt% Co–$BaCO_3$ catalysts had the reducible Co^{4+}–O species ($BaCoO_3$), which proceeded redox cycle with ethane and CO_2 in ODE with CO_2. In contrast, $BaCO_3$ did not show any H_2 reduction peaks and it was almost inactive in ODE with CO_2. The difference in the activation energy suggests that active sites and reaction pathways on 7 wt% Co–$BaCO_3$ catalyst are different from those on $BaCO_3$. These findings indicate that catalytic reactivity of Co–$BaCO_3$ catalysts is close associated with the presence of Co^{4+}–O species. These reducible Co^{4+}–O species are main active sites for ODE with CO_2, and oxidative dehydrogenation is major reaction pathway on Co–$BaCO_3$ catalysts in the reaction. The high redox property of Co–$BaCO_3$ catalysts favors conversion of ethane and CO_2 in the reaction, however, the much stronger redox property of these catalysts results in the deep oxidation of ethene. The characterization results demonstrate that the redox property of Co–$BaCO_3$ catalyst became stronger and stronger with the increase of Co content. Thus, ethane conversion and CO_2 conversion increased while ethene selectivity decreased on Co–$BaCO_3$ catalyst as Co content increasing.

On the other hand, Dang *et al.* [32–33] and Au *et al.* [34–36] found that $BaCO_3$ enhanced the catalytic activity of the catalysts in oxidation dehydrogenation of ethane and oxidative coupling of methane. For example, Dang *et al.* [33] reported that V-$BaCO_3$ catalysts showed high activity in oxidative dehydrogenation of ethane to ethene, due to the co-operation of $BaCO_3$ and $Ba_3(VO_4)_2$. Au *et al.* [34] found that $BaCO_3$ promoted the catalytic activity of $BaCO_3$/LaOBr catalyst in oxidative coupling of methane. The addition of $BaCO_3$ into the catalyst readily formed defects centers and trapped electrons on the catalyst, which enhanced the formation of active oxygen species. In the case of Co–$BaCO_3$ catalysts, the catalysts were composed of $BaCO_3$ and $BaCoO_3$. Therefore, the co-operation of $BaCO_3$ and $BaCoO_3$ is one of possible reasons for the high catalytic performance of Co–$BaCO_3$ catalysts in ODE with CO_2.

4. Conclusion

Co–$BaCO_3$ catalysts exhibited high catalytic performance in ODE with CO_2. The maximal formation rate of C_2H_4 was $0.264\ \text{mmol}\cdot\text{min}^{-1}\cdot(\text{g}\cdot\text{cat.})^{-1}$ (48.0% C_2H_6 conversion, 92.2% C_2H_4 selectivity, 44.3% C_2H_4 yield) on 7 wt% Co–$BaCO_3$ catalyst at 650 °C and $6000\ \text{ml}\cdot(\text{g}\cdot\text{cat})^{-1}\cdot\text{h}^{-1}$. The presence of Co–O species modified the properties of Co–$BaCO_3$ catalysts, which in turn determined the catalytic performance of these catalysts in ODE with CO_2. Co^{4+}–O species are main active sites on Co–$BaCO_3$ catalysts in the reaction. The redox cycle of Co–O species plays great roles on the catalytic performance of Co–$BaCO_3$ catalysts. On the other hand, the co-operation of $BaCO_3$ and $BaCoO_3$ is one of possible reasons for the high catalytic activity of these catalysts.

References

[1] M.C.J. Bradford and M.A. Vannice, Catal. Rev. Sci. Eng. 41 (1991) 1.
[2] F.Z. Zhang and B.Q. Xu, Prog. Chem. 14 (2002) 54.
[3] X. Ge and J.Y. Shen, Chem. J. Chin. Univ. 22(12) (2001) 2085.
[4] K. Nakagawa, M. Okamura, N. Ikenaga, T. Suzuki and T. Kobayashic, J. Chem. Soc. Chem. Comm. (1998) 1025.
[5] N. Kiyoharu, K. Chiaki and I. Yuichiro, Catal. Lett. 64 (2000) 215.
[6] O.V. Krylov, A.Kh. Mamedov and S.R. Mirzabekova, Catal. Today 24 (1995) 371.
[7] S. Wang, K. Murata, T. Hayakawa and K. Suzuki, Catal. Lett. 63 (1999) 59.
[8] S. Wang, K. Murata, T. Hayakawa and K. Suzuki, Appl. Catal. A. 156 (2000) 1.
[9] L. Xu, L. Lin and Q. Wang, et al., Stud. Surf. Sci. Catal. 119 (1998) 605.
[10] X. Ge, M. Zhu and J. Shen, React. Kinet. Catal. Lett. 77(1) (2002) 103.
[11] S.R. Mizabekova, A.Kh. Mamedov and V.S. Aliev, React. Kinet. Catal. Lett. 47(2) (1992) 159.
[12] S.R. Mizabekova, A.Kh. Mamedov and O.V. Krylov, Kinet. Katal. 38(5) (1997) 651.
[13] S. Nishama, Y. Sasaki and H. Okada, JP 05 170 673, 1993.
[14] L. Xu, J. Liu and H. Yang, Catal. Lett. 62 (1999) 185.
[15] L. Xu, S. Zhang and Q. Wang, CN 1 181 993A, 1998.
[16] Y. Liu, J. Xue, X. Liu and S.B. Li, Stud. Surf. Sci. Catal. 119 (1998) 593.
[17] F. Solymosi and R. Nemeth, Catal. Lett. 62 (1999) 197.
[18] R.X. Valenzuela, G. Bueno, V.C. Corberan, Y.D. Xu and C. Chen, Catal. Today 61 (2000) 43.
[19] R.X. Valenzuela, G. Bueno, A. Sobles, F. Sapina, E Martinez and V. Cortes Corberan, Catal. Lett. 15(3/4) (2001) 181.
[20] N. Mimura, I. Takahara, M. Inaba, M. Okamoto and K. Murata, Catal. Comm. 3 (2002) 257.
[21] Y.L. Bi, V.C. Corberan, H. Zhuang and K.J. Zhen, Stud. Surf. Sci. Catal. 153 (2004) 343.
[22] X. Zhao and X. Wang, Catal. Comm. 7 (2006) 633.
[23] Yu.I. Pyatuisky, N.L. Ilcherko and L.N. Raevskaya, Stud. Surf. Sci. Catal. 130 (2000) 707.
[24] H.X. Dai, C.F. Ng and C.T. Au, Stud. Surf. Sci. Catal. 130 (2000) 1757.
[25] T. Sekiya, N. Mochida and A. Ohtsuka, J. Non-crystal. Solids 168 (1994) 106.
[26] G. Mestl, M.P. Rosynek and J.H. Lunsford, J. Phys. Chem. B 101 (1997) 9321.
[27] G. Mestl, M.P. Rosynek and J.H. Lunsford, J. Phys. Chem. B 101 (1997) 9329.
[28] P. Pasierb, S. Komorniki, M. Rokita and M. Rekas, J. Mol. Struct. 596 (2001) 515.
[29] C.N.R. Rao, *Chemical Application of Infrared spectroscopy* (Academic Press, New York, 1963) 337.
[30] V.G. Milt, M.A. Ulla and E.E. Miro, Appl. Catal. B 57 (2005) 13.
[31] M. Rössel, H.R. Höche, H.S. Leipner, D. Völtzke, H.P. Abicht, O. Hollricher, J. Müller and S. Gablenz, Anal. Bioanal. Chem. 380 (2004) 157.
[32] Z. Dang, J. Gu, J. Lin, D. Yang and J. Chem. Soc. Chem. Comm. (1996) 1901.
[33] Z. Dang, J. Gu, J. Lin and D. Yang, Catal. Lett. 54 (1998) 129.
[34] C.T. Au, H. He, S.Y. Lai and C.F. Ng, J. Catal. 163 (1996) 399.
[35] C.T. Au, Y.Q. Zhang, H. He, S.Y. Lai and C.F. Ng, J. Catal. 167 (1997) 354.
[36] C.T. Au, K.D. Chen and C.F. Ng, Appl. Catal. A. 107 (1998) 81.